Enhancing selectivity of infrared emitters through quality-factor matching

Enas Sakr[a], Zhiguang Zhou[a], Peter Bermel[*a]

[a]Purdue University, School of Electrical & Computer Engineering, 1205 W State St., West Lafayette, IN, USA 47906

ABSTRACT

It has recently been proposed that designing selective emitters with photonic crystals (PhCs) or plasmonic metamaterials can suppress low-energy photon emission, while enhancing higher-energy photon emission. Here, we will consider multiple approaches to designing and fabricating nanophotonic structures concentrating infrared thermal radiation at energies above a critical threshold. These are based on quality factor matching, in which one creates resonant cavities that couple light out at the same rate that the underlying materials emit it. When this quality-factor matching is done properly, emissivities can approach those of a blackbody, but only within a selected range of thermal photon energies. One potential application is for improving the conversion of heat to electricity via a thermophotovoltaic (TPV) system, by using thermal radiation to illuminate a photovoltaic (PV) diode. In this study, realistic simulations of system efficiencies are performed using finite-difference time domain (FDTD) and rigorous coupled wave analysis (RCWA) to capture both thermal radiation and PV diode absorption. We first consider a previously studied 2D molybdenum photonic crystal with a commercially-available silicon PV diode, which can yield TPV efficiencies up to 26.2%. Second, a 1D-periodic samarium-doped glass emitter with a gallium antimonide (GaSb) PV diode is presented, which can yield efficiencies up to 38.5%. Finally, a 2D tungsten photonic crystal with a 1D integrated, chirped filter and the GaSb PV diode can yield efficiencies up to 38.2%; however, the fabrication procedure is expected to be more challenging. The advantages and disadvantages of each strategy will be discussed.

Keywords: infrared sources, infrared receivers, photonic crystals, thermophotovoltaics, thermal radiation, quality-factor matching

1. INTRODUCTION

Despite tremendous recent advances in energy technology, 61% of raw energy inputs (e.g., coal) burned in the US was rejected as waste heat last year [1]. If all this waste heat could instead be used to drive the efficient generation of electricity, it would fundamentally reshape the US energy landscape: reducing or eliminating energy imports, while reducing environmental damage at home. Also, a great number of new applications would open up, including handheld portable power generators, never-off generators using naturally-occurring steady heat sources, and solar power with integrated storage.

Incumbent technologies for harvesting waste heat are approaching performance limits, but solid-state technologies like photon-enhanced thermionic emission (PETE) [2] and thermophotovoltaics (TPV) [3] have great potential. Efficiencies over 40% are possible even at the previously examined temperatures of 970 ºC, and over 50% should be accessible at 1200 °C. However, conversion efficiencies depend strongly on selective control of infrared emission to augment their performance and approach these limits, which has not yet been achieved in experiment. Traditionally, thermal radiation is linked closely to choosing naturally selective materials. However, high temperatures and mediocre selectivity are the

[*] pbermel@purdue.edu; phone 765-496-7879; fax 765-494-4731; http://web.ics.purdue.edu/~pbermel/

norm in this case. Introducing materials with nanoscale structure can greatly impact the optical photon density of states, and would thus be expected to also strongly impact the performance of thermal radiative emitters. Several materials have been recently proposed for selective thermal emission, including photonic crystals (PhCs) and filters, nanoscale-gap emitter-receiver systems, rare earth materials, and refractory plasmonic metamaterials. Thus, the gap between prior and future experimental performance could be closed by combining appropriate choice of materials with geometry to achieve unprecedented control of thermal emission.

An effective approach for achieving improved selective thermal emission is to adjust the rate at which photons enter the cavity, so that it can match the rate of absorption, which is known as Q-matching. This in principle can allow up to 100% emissivity at selected wavelengths. The net effect of Q-matching in suitable materials is to create a strong contrast between the high emissivity regions just above the bandgap, and the low emissivity regions below. Photonic crystals, which are complex dielectric structures repeating periodically in one or more dimensions [4], have a well-demonstrated potential for high performance in TPV applications [5]. The most well-known characteristic of PhCs is the photonic bandgap: a range of frequencies where transmission can be strongly attenuated. This effect may also increase absorption outside of the photonic bandgap. Thus, the PhC enables conversion of heat to electricity by enhancing selective thermal emission at shorter wavelengths to increase the electrical output. Shawn-Yu Lin *et al*. have proven that 3D photonic crystal bandgaps can suppress thermal emission at longer wavelengths [6]. Similarly, 2D arrays of metallic photonic crystal microcavities can create strongly selective thermal emission, with emissivities above 90% [7] [5], [8], [9]. However, 2D and 3D metallic photonic crystals can pose challenges in terms of costs and scalability.

In an alternative approach, one may use external photon recycling of long-wavelength emission to improve efficiencies. For example, a rugate filter may be introduced on top of the photovoltaic (PV) diode to send unwanted long-wavelength photons back to the source, further improving the efficiency. Furthermore, residual low energy emission can be further reduced by the use of PhC filters, including plasma filters [3], quarter wave stacks [10] and rugate filters [11], [12]. These filters essentially reflect the low-energy photons back to the selective emitter, in a process known as “photon recycling” [12]–[16]. In order to achieve sufficient photon recycling, close proximity between the emitter and filter is required [15]. This requirement can be quantified by the view factor, which is the probability that emitted photons reach the PV receiver.

The combined effect of the innovations of Q-matching and selective filters has been calculated to yield efficiencies reaching as high as 26.9% with a molybdenum emitter at 1200 °C with a silicon PV diode, or 35.2% with a tungsten emitter at the same temperature using a GaSb PV diode. The best experimental results to date are consistent with this hypothesis, suggesting a 23% conversion of radiated thermal energy into electricity at a slightly lower temperature of 1050 °C.

However, Q-matching can be applied more broadly than just in metallic photonic crystal microcavities; recently work has shown that it can also improve rare-earth doped emitters. Here, narrow atomic transition lines associated with isolated dopants in a transparent substrate having a high melting point have their emissivity amplified through a surrounding photonic structure [17]. For example, the emission spectrum for samarium already displays peaks at wavelengths associated with high-performance TPV systems. Using samarium as a base, we may then achieve an emissivity close to 100% at selected wavelengths through the process of quality factor matching with metamaterials. Recent work already shows that the unique optical properties of wavelength-tunable metamaterials could wholly transform typical blackbody emission spectra [5], [6], [8], [18]–[20]; this makes them a particularly appropriate choice to drive highly-efficient TPV and PETE conversion processes. At the same time, due to the relative transparency of the fused silica, longer wavelengths outside the targeted range of enhancement would have near-zero emissivity, thus solving the most common flaw in other metamaterial-based designs. Using this approach to suppress long-wavelength and enhance short-wavelength emission in our system could improve TPV radiative efficiency by an order of magnitude at 1200 °C [5]. PETE could also greatly benefit from this approach to enhancing high-energy internal photon emission (e.g., for operating without an external source of photons like the sun, especially at night) [21].

Early work on rare-earth doped crystals, a naturally occurring material, demonstrated that some materials naturally demonstrate selective thermal emission. For example, an eightfold increased degree of selectivity in erbium aluminum garnet (ErAG) was caused by the natural atomic transitions of erbium in the near-infrared [22]. Similarly, doping fused silica glass with rare earth elements (e.g., erbium, samarium, and thulium) has been shown to yield narrowband absorption and emission lines in their spectra. An example of a selective thermal emitter based on rare-earth oxides was investigated in Bitnar's work [23]. Another example based on rare-earth ceramic selective emitters was investigated in Chubb's work [22], [24], in which ErAG was shown to have the largest extinction coefficient at 1.47 µm and 1.53 µm; hence, by Kirchoff's law of thermal radiation, an optically-thick ErAG film on a Platinum substrate produced selective spectral emittance around 1.5 µm at a substrate temperature of 1635K. However, the radiative efficiency alone was as low as 20% at a substrate temperature of 1635 K [22], and a significant parasitic long-wavelength emission tail was present, despite the very low extinction coefficient of the ErAG in the range from 2 µm to 5 µm. This is mainly caused by the use of a thick ErAG film to achieve high emittance at shorter wavelengths, as well as Ohmic losses from the platinum substrate.

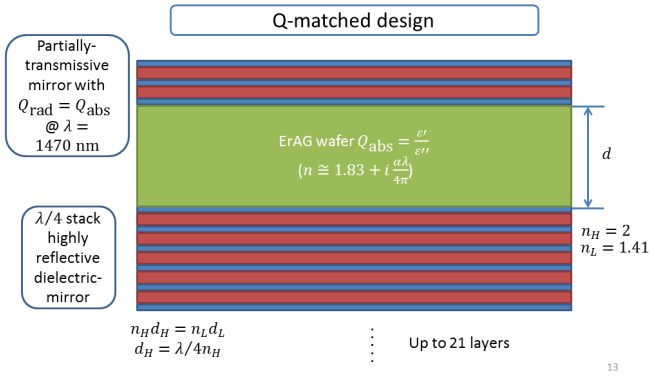

Figure 1: Rare earth-based selective thermal emitter (erbium aluminum garnet), using quality-factor matching to enhance relative emission at target wavelengths close to the blackbody limit (adapted from Ref. [25]).

Recent work from our group has shown that introducing an emitter structure into ErAG as shown in Fig. 1 both enhances emission for energies above the bandgap and suppresses emission below the bandgap [25]. It is also top-surface emitting, so that emission is directed almost exclusively towards a single set of PV cells above. This can be achieved using a high-temperature-tolerant dielectric mirror [26] as a substrate and a partially transmissive dielectric mirror on top of the ErAG film. Following previous work [27], the loss rate in the ErAG is matched to the loss rate of the partially transmissive dielectric mirror on top of the structure to achieve Q-matching and near-blackbody emissivity. Furthermore, an exponentially chirped multi-layer dielectric filter can be placed on top of the film to suppress a significant part of the sub-bandgap emission, while transmitting above-bandgap photons [5]. The proposed ErAG emitter is suitable for operation with GaSb PV cells. Assuming reasonable PV cell performance, the theoretical TPV efficiency is shown to reach 34% if the chirped filter emitter is used with a cold-side rugate filter with shifted cut-off to minimize losses beyond 3.5 µm. The TPV efficiency also reaches 33% if the chirped filter emitter design is used without any external filters. Such a multi-layer structure can be fabricated using sputter deposition technology [28] [29]–[31].

These highly selective thermal emitter materials need not be naturally occurring, either. Recent work from Vlad Shalaev's group has suggested the potential of plasmonic metamaterials operating at refractory temperatures to meet or exceed previously demonstrated levels of performance [20]. Thus, it stands to reason that combining naturally occurring enhanced emission wavelengths with metamaterial surfaces would yield the best possible thermal emission performance with just a few material layers. In the following sections, we discuss our methodology for calculating the emission selectivity and TPV system efficiency, and then compare the performance of two distinctive designs.

2. METHODS

Physics-based modeling and simulation of the optical, thermal, and mechanical properties of the system allows us to predict the performance of each selective emitter design, and then optimize our structure subject to fabrication constraints such as materials availability and control and length of deposition. We expect this approach to yield a set of emittance peaks in the targeted range of wavelengths for our projected applications.

The performance of TPV system with photonic crystal emitters made by various refractory metals is simulated with the TPXsim simulation tool. The TPXsim tool is an integrated simulation tool developed to simulate the efficiency of the entire TPV system as a whole, using the nanoHUB Rappture software development tool to combine all the calculations into a single interface; it is closely based on its predecessor, TPVtest [32]. The optical performance of the selective emitter structure in Fig. 1 – specifically, the transmission and reflection spectra – is calculated using a coupled wave analysis and scattering matrix tool for solving Maxwell's equations, known as S4 [33], [34] [42]. By Kirchoff's law for bodies in thermal equilibrium, the absorptivity equals the emissivity – our desired result [35]. Next, we employ a compact model to solve the electrical performance of the TPV diode receiver. Various recombination mechanisms can be considered in this framework, including the bulk SRH, surface, Auger, and radiative recombination. Radiative recombination is the most fundamental source of losses, present in any piece of material at a finite temperature. In a homogeneous environment, it is related to the absorption coefficient by the Roosbroeck-Shockley equation [36], which allows us to use our electromagnetic simulation framework to predict enhancement of the radiative recombination rate in a self-consistent manner. The overall power conversion efficiency of the TPV diode is given by [37]:

$$\eta = \frac{J_{sc} \cdot V_{oc} \cdot FF}{P_{emit}} \tag{1}$$

where V_{oc} is the open-circuit voltage, J_{sc} is the short-circuit current, FF is the fill-factor, and P_{emit} is the total emitted thermal power per unit area. The open circuit voltage is given by [38]:

$$qV_{oc} = E_g - nk_BT \ln\left(\frac{A}{J_{sc}}\right), \tag{2}$$

where E_g is the bandgap of the PV material, n is the ideality factor, q is the elementary charge, k_B is the Boltzmann constant, T is the temperature, and A is the recombination term, consisting of radiative recombination and Shockley-Read-Hall recombination mechanisms, given by [39], [40]:

$$A = \frac{q(\varepsilon + 1)E_g^2\, k_BT}{4\pi^2\hbar^3c^2} + \frac{4qD}{L_DN_D}\left(\frac{k_BT\sqrt{m_e^*m_h^*}}{2\pi\hbar^2}\right)^3, \tag{3}$$

where ε is the dielectric permittivity, $\hbar$ is Planck's constant, c is the speed of light, D is the diffusion coefficient, L_D is the diffusion length, N_D is the defect density, and m_e^* and m_h^* are the effective masses for electrons and holes, respectively. In general, additional terms such as Auger recombination can be added in the presence of high injection currents. The dark current is then given by $J_s = Ae^{-E_g/nk_BT}$. The fill factor FF can be estimated as FF_{sh}, which can be calculated in three steps [37]:

$$FF_o = \frac{z_{oc} - \ln(z_{oc} + 0.72)}{z_{oc} + 1} \tag{4a}$$

$$FF_s = FF_o[1 - 1.1r_s] + 0.185r_s^2 \tag{4b}$$

$$FF_{sh} = FF_s\left[1 - \left(\frac{V_{oc} + 0.7}{V_{oc}}\right)\frac{FF_s}{r_{SH}}\right], \tag{4c}$$

where $z_{oc} = qV_{oc}/nk_BT$ is the reduced open-circuit voltage, $r_s = I_{sc}R_s/V_{oc}$ is the reduced series resistance, and $r_{sh} = I_{sc}R_{sh}/V_{oc}$ is the reduced shunt resistance. The short circuit current J_{sc} is given by:

$$J_{sc} = \int_0^{\infty} d\lambda \, \frac{2qc}{\lambda^4} \frac{\varepsilon(\lambda) EQE(\lambda)}{\exp(hc/\lambda kT) - 1}, \tag{5}$$

where q is the electron charge, c is the speed of light in vacuum, λ is the wavelength, $\varepsilon(\lambda)$ is the spectral emittance of the emitter, $EQE(\lambda)$ is the external quantum efficiency of the device, V is the voltage, and T_d is the device temperature.

3. RESULTS AND DISCUSSION

In this section, we consider the two types of selective thermal emitter designs driven by quality-factor matching mentioned in the introduction – namely, rare earth-doped selective emitters sandwiched between two multilayer stacks, as shown in Fig. 1, and tungsten photonic-crystal based selective emitters integrated with chirped quarter wave stack filters, as shown in Fig. 7.

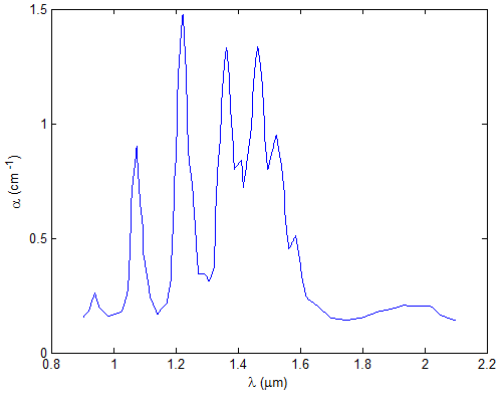

Figure 2: The absorption spectrum for rare earth samarium-doped fused silica demonstrates that its material properties offer a close match to the wavelengths needed for efficient radiation of heat in the near-infrared.

To understand the value of a rare earth-doped emitter, it is instructive to first consider its basic material properties in the absence of quality-factor matching. The baseline emission spectrum for the material shown in Fig. 2 demonstrates that the inherent selectivity of samarium-doped glass is on the order of a factor of eight, with wavelengths around 1.5 μm showing emissivity of approximately 80% for a wafer-based 5 mm sample, and approximately 10% over a broad range of wavelengths from 2-4 μm. Preliminary results in Fig. 3 show the introduction of the 1D layer structures on the top and

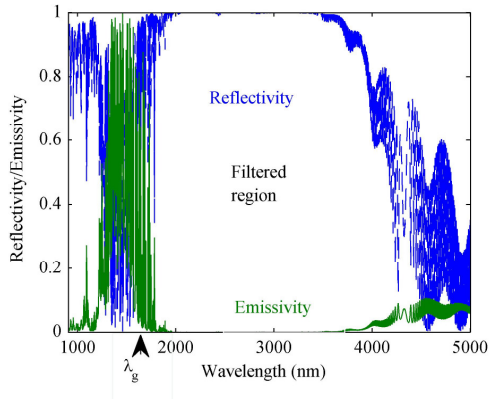

Figure 3: Combining a rare earth samarium-doped fused silica emitter with a metamaterial reflector enhances near-infrared emission, while strongly suppressing parasitic losses through filtering. Overall spectral emission efficiency is 84.5% at 1300 °C.

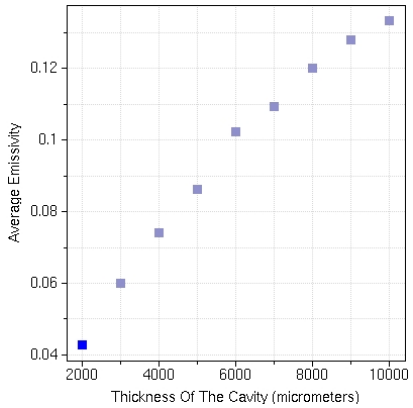

Figure 4: The average emissivity of the rare earth samarium-doped fused silica emitter (compared to a blackbody) increases almost linearly with the glass thickness, up to values approaching 1 cm.

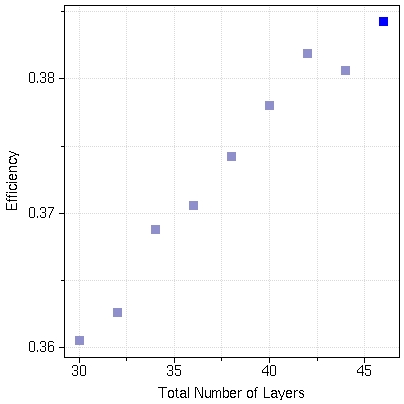

Figure 5: Adding more layers can gradually push TPV conversion efficiencies linearly, up from the baseline value toward at least 38.5% for 47 layers (using a thickness of 6 mm).

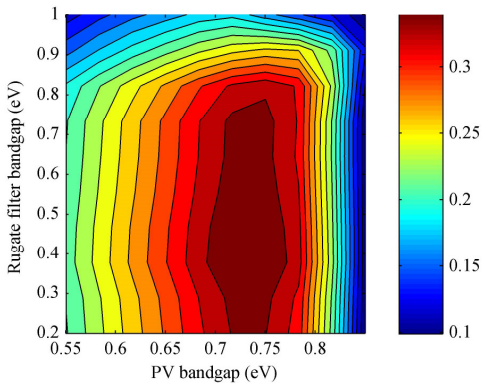

Figure 6: TPV efficiency for the Q-matched erbium aluminum garnet (ErAG) substrate with a chirped filter, as a function of the PV diode bandgap (x-axis) and the rugate filter bandgap (y-axis). Maximum efficiencies reach approximately 34% [27].

bottom can induce a doubling of the overall emission efficiency, up to a value of 78% at 1200 °C, which itself is an improvement by nearly an order of magnitude over a standard blackbody source of equal temperature. The associated

TPV efficiency using 26 cladding layers would be 35.6%, with an average emissivity of 8.6% compared to a blackbody.

Furthermore, the performance of rare earth-doped emitters can be fine-tuned through adjustment to key parameters, while still using the same underlying materials. For example, as shown in Fig. 4, increasing the thickness of the glass layer can increase the emissivity almost linearly with thickness, from 4.1% to 13.2%, over thicknesses that range from 2 mm up to 1 cm, values commonly used in smaller glass objects. Also, Fig. 5 illustrates that increasing the number of layers surrounding the glass results in improved efficiencies: as high as 38.5% for 46 layers at 1300 °C.

By comparison, earlier investigations on erbium aluminum garnet show a slightly lower maximum efficiency of approximately 34% at 1300 °C [25]. As shown in Fig. 6, varying the PV bandgap (x-axis) or the rugate filter bandgap (y-axis) cannot achieve a large improvement in this previously calculated performance. This suggests that samarium-doped glass may be a somewhat preferable option for rare earth-doped selective emitters.

Finally, we consider a much different structure, shown in Fig. 7, in which the previously-investigated tungsten photonic crystal is integrated directly with a quarter wave stack filter consisting of up to 15 bilayers of silicon dioxide and titanium dioxide. Such an approach has the advantage of maximizing the view factor between the thermal emitter and the filter. However, there are potential disadvantages associated with the use of a high-index medium for the quality-factor matched tungsten holes, which may partially offset these advantages. In order to investigate this phenomenon, we used the finite-difference time domain tool known as MEEP [41] to simulate the absorption profile of this structure, as shown in Fig. 8(a) as a function of the number of chirped quarter wave stack bilayers. It is evident that increasing the number of bilayers was only helpful up to a certain point, because of higher order reflections which suppress useful emission. The parasitic emission modes shown in Fig. 8(b)-(d) also create a practical limit on emitter efficiency. Combined with emission in the long wavelength infrared (not shown), the overall efficiency can reach up to 38.2% -- higher than the

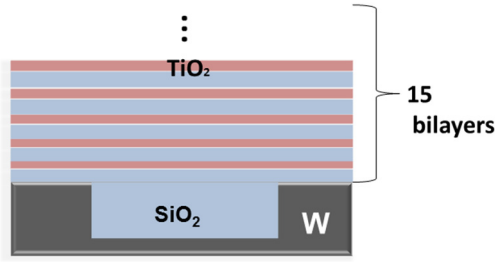

Figure 7: Schematic showing a cross-section of a tungsten photonic crystal combined with a multilayer quarter wave stack. This structure has potential to achieve higher efficiencies with a near-unity view factor to enhance photon recycling.

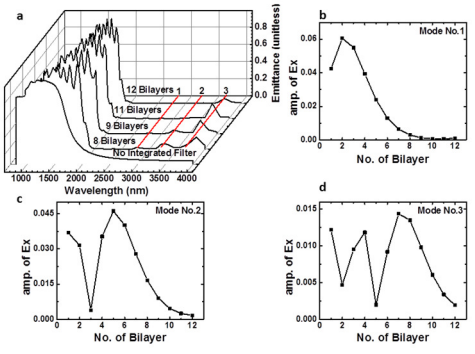

Figure 8: Results for the tungsten photonic crystal combined with a quarter wave stack filter shown in Fig. 7: (a) emission spectra from 1-4 μm for various numbers of bilayers and (b)-(d) field profiles of parasitic emission modes denotes by lines 1-3 in (a).

value of 35.2% predicted in the absence of the integrated filter.

By comparison, it can be seen in Fig. 9 that varying the geometry of molybdenum-based selective emitters (e.g., the depth) does not yield a significant increase in performance compared to previous work, with maximum efficiencies of 26.2% for depths of 1 μm or greater. This is because the quality factor of an emitter using this material is too low to fully suppress a substantial amount of parasitic emission beyond the band edge of crystalline silicon at 1.107 μm. This result shows the value of using either more inherently selective materials (such as rare earths) or mimicking their properties using other mechanisms, such as integrated filters.

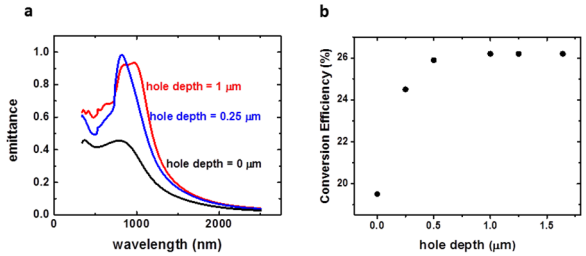

Figure 9: Performance of the Mo-based 2D PhC selective emitter with varying input parameters (a) emissivity spectrum for three different hole depths (b) efficiency as a function of hole depth. The latter saturates for depths over 1 μm.

4. CONCLUSIONS

In conclusion, quality-factor matching is a critical strategy for enhancing the selectivity of infrared thermal emission. Particularly in applications where only photons above a certain cutoff can be utilized, such as thermophotovoltaics or photon-enhanced thermionic emission, it can lead to substantial improvements in performance. Previous work found that materials with only weak inherent selectivity, such as molybdenum or tungsten, placed into 2D photonic crystals can achieve TPV efficiencies up to 26.2% with molybdenum emitters and silicon PV diodes, or 35.2% with tungsten emitters and GaSb diodes at 1300 °C. For materials with stronger inherent selectivity, such as samarium-doped glasses, the effect of quality-factor matching can be even stronger, with calculated efficiencies potentially reaching up to 38.5% at 1300 °C. Similar performance up to 38.2% can also be achieved at the same temperature by improving on the previous 2D tungsten photonic crystal by integrating a quarter wave stack filter. This effect can also be viewed as mimicking the benefits of more inherently selective materials.

ACKNOWLEDGMENTS

Support was provided by the Department of Energy, under DOE Cooperative Agreement No. DE-EE0004946 (PVMI Bay Area PV Consortium), the Semiconductor Research Corporation, under Research Task No. 2110.006 (Network for Photovoltaic Technologies), and the National Science Foundation, under Award EEC1454315-CAREER: Thermophotonics for Efficient Harvesting of Waste Heat as Electricity.

REFERENCES

[1] L. L. N. Laboratory, “2013 US Energy Flowchart,” *LLNL-MI-410527*, 2014. [Online]. Available: https://flowcharts.llnl.gov/energy.html#2013.

[2] J. W. Schwede, T. Sarmiento, V. K. Narasimhan, S. J. Rosenthal, D. C. Riley, F. Schmitt, I. Bargatin, K. Sahasrabuddhe, R. T. Howe, J. S. Harris, N. a Melosh, and Z.-X. Shen, “Photon-enhanced thermionic emission from heterostructures with low interface recombination.,” *Nat. Commun.*, vol. 4, p. 1576, 2013.

[3] B. Wernsman, R. R. Siergiej, S. D. Link, R. G. Mahorter, M. N. Palmisiano, R. J. Wehrer, R. W. Schultz, G. P. Schmuck, R. L. Messham, S. Murray, C. S. Murray, F. Newman, D. Taylor, D. M. Depoy, and T. Rahmlow, "Greater Than 20% Radiant Heat Conversion Efficiency of a Thermophotovoltaic Radiator/Module System Using Reflective Spectral Control," *IEEE Trans. Electron Devices*, vol. 51, pp. 512–515, Mar. 2004.

[4] J. D. Joannopoulos, S. G. Johnson, J. N. Winn, and R. D. Meade, *Photonic Crystals: Molding the Flow of Light*, 2nd ed. Princeton, NJ: Princeton, 2008.

[5] P. Bermel, M. Ghebrebrhan, W. Chan, Y. X. Yeng, M. Araghchini, R. Hamam, C. H. Marton, K. F. Jensen, M. Soljacic, J. D. Joannopoulos, S. G. Johnson, and I. Celanovic, "Design and global optimization of high-efficiency thermophotovoltaic systems," *Opt. Express*, vol. 18, pp. A314–A334, 2010.

[6] S.-Y. Lin, J. G. Fleming, D. L. Hetherington, B. K. Smith, R. Biswas, K. M. Ho, M. M. Sigalas, W. Zubrzycki, S. R. Kurtz, and J. Bur, "A three-dimensional photonic crystal operating at infrared wavelengths," *Nature*, vol. 394, pp. 251–253, 1998.

[7] M. Ghebrebrhan, Y.-X. Yeng, P. Bermel, I. Celanovic, M. Soljacic, and J. D. Joannopoulos, "Tailoring thermal emission via Q-matching of photonic crystal resonances," *Phys. Rev. A*, vol. 83, p. 33810, 2011.

[8] Y. X. Yeng, M. Ghebrebrhan, P. Bermel, W. R. Chan, J. D. Joannopoulos, M. Soljacic, and I. Celanovic, "Enabling high-temperature nanophotonics for energy applications," *Proceedings of the National Academy of Sciences*, vol. 109. pp. 2280–2285, 2012.

[9] P. Bermel, M. Ghebrebrhan, M. Harradon, Y. X. Yeng, I. Celanovic, J. D. Joannopoulos, and M. Soljacic, "Tailoring photonic metamaterial resonances for thermal radiation.," *Nanoscale Res. Lett.*, vol. 6, no. 1, p. 549, 2011.

[10] J. N. Winn, Y. Fink, S. Fan, and J. D. Joannopoulos, "Omnidirectional reflection from a one-dimensional photonic crystal," *Opt. Lett.*, vol. 23, pp. 1573–1575, 1998.

[11] B. G. Bovard, "Rugate filter theory: an overview.," *Appl. Opt.*, vol. 32, pp. 5427–5442, 1993.

[12] U. Ortabasi and B. Bovard, "Rugate technology for thermophotovoltaic applications: a new approach to near perfect filter performance," *AIP Conf. Proc.*, vol. 653, pp. 249–258, 2003.

[13] F. O'Sullivan, I. Celanovic, N. Jovanovic, J. Kassakian, S. Akiyama, and K. Wada, "Optical characteristics of 1D Si/SiO2 photonic crystals for thermophotovoltaic applications," *J. Appl. Phys.*, vol. 97, p. 33529, 2005.

[14] R. E. Black, P. F. Baldasaro, and G. W. Charache, "Thermophotovoltaics - development status and parametric considerations for power applications," in *International Conference on Thermoelectrics*, 1999, vol. 18, pp. 639–644.

[15] A. Heinzel, V. Boerner, A. Gombert, B. Blasi, V. Wittwer, and J. Luther, "Radiation filters and emitters for the NIR based on periodically structured metal surfaces," *J. Mod. Opt.*, vol. 47, 2000.

[16] P. M. Fourspring, D. M. DePoy, T. D. Rahmlow, J. E. Lazo-Wasem, and E. J. Gratrix, "Optical coatings for thermophotovoltaic spectral control.," *Appl. Opt.*, vol. 45, pp. 1356–1358, 2006.

[17] M. R. Khan, X. Wang, P. Bermel, and M. A. Alam, "Enhanced light trapping in solar cells with a meta-mirror following generalized Snell's law," *Opt. Express*, vol. 22, p. A973, 2014.

[18] W. Cai and V. Shalaev, *Optical metamaterials: Fundamentals and applications*. 2010, pp. 1–200.

[19] S. Y. Lin, J. Moreno, and J. G. Fleming, "Three-dimensional photonic-crystal emitter for thermal photovoltaic power generation," *Appl. Phys. Lett.*, vol. 83, pp. 380–382, 2003.

[20] U. Guler, A. Boltasseva, and V. M. Shalaev, "Refractory Plasmonics," *Science (80-.).*, vol. 344, pp. 263–264, 2014.

[21] J. W. Schwede, I. Bargatin, D. C. Riley, B. E. Hardin, S. J. Rosenthal, Y. Sun, F. Schmitt, P. Pianetta, R. T. Howe, Z.-X. Shen, and N. A. Melosh, "Photon-enhanced thermionic emission for solar concentrator systems.," *Nat. Mater.*, vol. 9, pp. 762–767, 2010.

[22] D. L. Chubb, A. T. Pal, M. O. Patton, and P. P. Jenkins, “Rare earth doped high temperature ceramic selective emitters,” *Journal of the European Ceramic Society*, vol. 19. pp. 2551–2562, 1999.

[23] B. Bitnar, W. Durisch, J. C. Mayor, H. Sigg, and H. R. Tschudi, “Characterisation of rare earth selective emitters for thermophotovoltaic applications,” *Sol. Energy Mater. Sol. Cells*, vol. 73, pp. 221–234, 2002.

[24] A. Datas, D. L. Chubb, and A. Veeraragavan, “Steady state analysis of a storage integrated solar thermophotovoltaic (SISTPV) system,” *Sol. Energy*, vol. 96, pp. 33–45, 2013.

[25] E. Sakr, Z. Zhou, and P. Bermel, “High efficiency rare-earth emitter for thermophotovoltaic applications,” *Appl. Phys. Lett.*, vol. 105, p. 111107, 2014.

[26] C. K. Carniglia and J. H. Apfel, “Maximum reflectance of multilayer dielectric mirrors in the presence of slight absorption,” *J. Opt. Soc. Am.*, vol. 70, pp. 523–534, 1980.

[27] I. Celanovic, D. Perreault, and J. Kassakian, “Resonant-cavity enhanced thermal emission,” *Phys. Rev. B*, vol. 72, p. 75127, 2005.

[28] K. Wasa and S. Hayakawa, *Handbook of sputter deposition technology : principles, technology, and applications*. 1992, p. xii, 304 p.

[29] M. Mazur, D. Kaczmarek, J. Domaradzki, D. Wojcieszak, P. Mazur, and E. Prociow, “Structural and surface properties of TiO2 thin films doped with neodymium deposited by reactive magnetron sputtering,” *Mater. Sci.*, vol. 31, pp. 71–79, 2013.

[30] O. Deparis, M. Rassart, C. Vandenbem, V. Welch, J. P. Vigneron, L. Dreesen, and S. Lucas, “Dielectric multilayer films fabricated by magnetron sputtering: How far can the iridescence be tuned?,” in *Plasma Processes and Polymers*, 2009, vol. 6.

[31] S. Chao, W. H. Wang, and C. C. Lee, “Low-Loss Dielectric Mirror with Ion-Beam-Sputtered TiO 2-SiO 2 Mixed Films.,” *Appl. Opt.*, vol. 40, pp. 2177–2182, 2001.

[32] Q. Chen, P. Bermel, R. Shugayev, M. Sumino, Z. Zhou, and O. Yehia, “TPV Efficiency Simulation.” 2013.

[33] V. Liu and S. Fan, “S4 : A free electromagnetic solver for layered periodic structures,” *Comput. Phys. Commun.*, vol. 183, no. 10, pp. 2233–2244, Oct. 2012.

[34] J. Kang, X. Wang, C. Liu, and P. Bermel, “S4: Stanford Stratified Structure Solver.” 2013.

[35] G. B. Rybicki and A. P. Lightman, *Radiative Processes in Astrophysics*. Weinheim, Germany: Wiley-VCH Verlag GmbH, 1985.

[36] W. Van Roosbroeck and W. Shockley, “Photon-radiative recombination of electrons and holes in germanium,” *Phys. Rev.*, vol. 94, pp. 1558–1560, 1954.

[37] M. A. Green, “Third generation photovoltaics: Ultra-high conversion efficiency at low cost,” *Prog. Photovoltaics Res. Appl.*, vol. 9, pp. 123–135, 2001.

[38] R. F. Pierret, “Semiconductor Device Fundamentals,” *New York*, p. 792, 1996.

[39] C. Kittel, *Introduction to solid state physics*. 2005, p. 703.

[40] C. H. Henry, “Limiting efficiencies of ideal single and multiple energy gap terrestrial solar cells,” *J. Appl. Phys.*, vol. 51, pp. 4494–4500, 1980.

[41] A. F. Oskooi, D. Roundy, M. Ibanescu, P. Bermel, J. D. Joannopoulos, and S. G. Johnson, “Meep: A flexible free-software package for electromagnetic simulations by the FDTD method,” *Comput. Phys. Commun.*, vol. 181, no. 3, pp. 687–702, 2010.